2D-IR Spectroscopy of an AHA Labeled Photoswitchable PDZ2 Domain

Stucki-Buchli, Brigitte ; Johnson, Philip J M ; Bozovic, Olga ; Zanobini, Claudio ; Koziol, Klemens L ; Hamm, Peter ; Gulzar, Adnan ; Wolf, Steffen ; Buchenberg, Sebastian ; Stock, Gerhard

Abstract: We explore the capability of the non-natural amino acid azidohomoalanine (AHA) as an IR label to sense relatively small structural changes in proteins with the help of 2D IR difference spectroscopy. To that end, we AHA-labeled an allosteric protein (the PDZ2 domain from human tyrosine-phosphatase 1E) and furthermore covalently linked it to an azobenzene-derived photoswitch as to mimic its conformational transition upon ligand binding. To determine the strengths and limitations of the AHA label, in total six mutants have been investigated with the label at sites with varying properties. Only one mutant revealed a measurable 2D IR difference signal. In contrast to the commonly observed frequency shifts that report on the degree of solvation, in this case we observe an intensity change. To understand this spectral response, we performed classical MD simulations, evaluating local contacts of the AHA labels to water molecules and protein side chains and calculating the vibrational frequency on the basis of an electrostatic model. Although these simulations revealed in part significant and complex changes of the number of intraprotein and water contacts upon trans-cis photoisomerization, they could not provide a clear explanation of why this one label would stick out. Subsequent quantum-chemistry calculations suggest that the response is the result of an electronic interaction involving charge transfer of the azido group with sulfonate groups from the photoswitch. To the best of our knowledge, such an effect has not been described before.

DOI: https://doi.org/10.1021/acs.jpca.7b09675

2D-IR Spectroscopy of an AHA Labelled Photoswitchable PDZ2 Domain

Brigitte Stucki-Buchli, Philip J. M. Johnson, Olga Bozovic,

Claudio Zanobini, Klemens L. Koziol, Peter Hamm*

Department of Chemistry, University of Zurich, Zurich, Switzerland

and

Adnan Gulzar, Steffen Wolf, Sebastian Buchenberg, Gerhard Stock*

Biomolecular Dynamics, Institute of Physics, Albert Ludwigs University, Freiburg, Germany

**corresponding authors:* peter.hamm@chem.uzh.ch and stock@physik.uni-freiburg.de

(Dated: November 19, 2017)

Abstract

Abstract: We explore the capability of the non-natural amino acid azidohomoalanine (AHA) as an IR label to sense relatively small structural changes in proteins with the help of 2D IR difference spectroscopy. To that end, we AHA-labelled an allosteric protein (the PDZ2 domain from human tyrosine-phosphatase 1E) and furthermore covalently linked it to an azobenzene-derived photoswitch as to mimic its conformational transition upon ligand binding. To determine the strengths and limitations of the AHA label, in total six mutants have been investigated with the label at sites with varying properties. Only one mutant revealed a measurable 2D IR difference signal. In contrast to the commonly observed frequency shifts which report on the degree of solvation, in this case we observe an *intensity* change. To understand this spectral response, we performed classical MD simulations, evaluating local contacts of the AHA labels to water molecules and protein side chains and calculating the vibrational frequency based on an electrostatic model. While these simulations revealed in part significant and complex changes of the number of intraprotein and water contacts upon *trans-cis* photoisomerization, they could not provide a clear explanation of why this one label would stick out. Subsequent quantum-chemistry calculations suggest that the response is the result of an electronic interaction involving charge transfer of the azido group with sulphonate groups from the photoswitch. To the best of our knowledge, such an effect has not been described before.

I. INTRODUCTION

Proteins are dynamical objects. The structural dynamics of proteins involve equilibrium processes, such as thermally driven fluctuation, as well as non-equilibrium processes, such as the conformational transition in a light-triggered protein. Vibrational spectroscopy provides an inherent picosecond time resolution to study both equilibrium and non-equilibrium processes. However, obtaining site-selective information from vibrational spectroscopy will in general require vibrational labels, since the IR spectrum of a molecule of that size is no longer resolved into its normal modes. Ideally, such vibrational labels should absorb outside of the congested region of the absorption spectrum of a protein[1–5] in order to discriminate it from a huge background. Various distinct molecular groups have been suggested for that purpose: –SH vibrations of cysteines,[6] –CD vibrations of deuterated amino acids,[7–9] –C≡O vibrations of metal-carbonyls either from natural cofactors such as a heme group[10–12] or from complexes that can be bound to amino acids in a post-translational step,[13–15] as well as –N_3,[16–22] –C≡N[23,24] and –SCN[25] vibrations from non-natural amino acids. All these molecular groups have in common that they absorb in a spectral window between ≈1700 cm^{-1} and ≈2800 cm^{-1}, where essentially no fundamental modes of natural proteins are found (with the one exception of the –SH vibrations of cysteines), and where the only background originates from the still quite strong but very broad and featureless absorption of the solvent water.

In addition to having a frequency in that spectral window, a good label should fulfill the following criteria:

- The extinction coefficient of the label should be large enough so that it can be detected at reasonable concentrations. As most proteins are not soluble at high concentrations, the goal is to measure at concentrations of around 1 mM or below. This concentration range is comparable to what is commonly used for NMR measurements.

- It should be versatile and incorporable at essentially any position of a protein with good yields and at a high purity (since IR measurements require large amounts of sample).

- It should not significantly perturb the structure and the stability of a protein.

- The label should be sensitive to its environment, e.g., sense the polarity or hydrophobicity of its surrounding.

With these criteria in mind, we currently concentrate on the non-natural amino acid azidohomoalanine (AHA) as a label, which contains an azido group ($-N_3$) that absorbs at around 2100 cm^{-1}. It has a reasonably high extinction coefficient of 300-400 $M^{-1}cm^{-1}$,[20] large enough to be measured at concentrations well in the sub millimolar regime by 2D IR spectroscopy.[4,22] As a small amino acid that is a methionine analog, it can be incorporated also into larger proteins (which can no longer be synthesized on a peptide synthesizer) at essentially any position by a methionine auxotrophic protein expression strategy.[26,27] It does not perturb protein properties very much, as evidenced for example by the fact that labelling a peptide ligand with AHA affects its binding affinity to a PDZ2 domain only to a small extent.[20] Finally, AHA has been shown to be a sensitive probe of its environment. For example, when AHA is buried in the hydrophobic core in the folded state,[17] the azido band blue-shifts by up to 20 cm^{-1} upon protein unfolding. Along the same lines, it can also be used to detect binding of an AHA-labelled peptide ligand to a larger protein, in which case the degree of solvation of the label diminishes, causing a red-shift of its vibration.[20,22] Such shifts have been explained mainly by changes in hydrogen bonding to the first and/or third nitrogen atom of the azido group as well as to variations in the angle between the hydrogen bond and the azido group.[21,28] Furthermore, the vibrational frequency is also influenced by the polarity of the environment,[21] e.g., Coulomb interactions to the middle nitrogen atom of the azido group can shift the vibration.[18]

In the present study, we explore the capability of the AHA label to sense relatively small structural changes of a protein, i.e., changes much smaller than those occurring upon unfolding. To that end, we employ a protein construct that we have designed and characterized recently, see Fig. 1.[29–32] That is, we have chosen the second PDZ (PDZ2) domain from human tyrosine-phosphatase 1E (hPTP1E), which has been studied extensively as a model allosteric protein from different perspectives, i.e., structural,[33–35] dynamical[36–38] or computational.[31,32,39–48] In order to investigate the allosteric mechanism by transient IR spectroscopy, we have covalently linked an azobenzene derivative across the binding groove of the PDZ2 domain in such a way that the light-driven *trans-cis* isomerization of the photoswitch induces a structural transition in the protein, which mimics ligand unbinding in the native system.[29] By NMR analysis (PDB entries: 2M0Z and 2M10), we have confirmed

that the structural changes, which are of the order of 1 Å, are of similar size as in the native system.

We have shown by transient IR spectroscopy that the protein responds to the light-induced perturbation on two timescales, one extending up to ≈100 ns that reflects the opening of the binding groove (which we know since luckily we could isolate one specific mode localized on the azobenzene derivative), and a second phase on a 10 μs timescale.[29] We have no information from experiment on the structural nature of the second phase, since we did not employ any label that would reveal site-selective information. Based on molecular dynamics (MD) simulations, we suggested that it involves some of the more flexible and remote loop regions of the protein and/or the termini.[31,32] MD simulations also suggested[29] that the water solvation shell changes on the timescale of the binding groove opening even relatively far away from the perturbation, and we proposed that both aspects (i.e., structural changes of regions far away from the binding groove and/or changes in solvation) might be possible mechanisms of allostery. Based on the experience from previous works employing AHA in other molecular systems,[17–22,28] it appears possible that this label can sense such effects in a photoswitchable PDZ2 domain, and it is the goal of the present paper to explore whether this is indeed possible.

As a first step in this direction, we consider stationary difference spectra comparing the two states of the protein, and leave time dependent transient experiments for a future publication. To explore the capability of the AHA label as a probe of the change of the local structure, the following criteria have been used to select the positions for the AHA label:

- Amino acids close (L78, N80, I20) *versus* far away (N16, S48, L66) from the photoswitch have been selected, in order to investigate the dependence on the distance from the perturbation.

- Amino acids within secondary structural elements (L78, S48) *versus* loop regions (N16, L66) have been selected. Whereas the PDZ2 domain undergoes only small shifts in the more rigid secondary structural elements, larger conformational changes can be observed in the flexible loops.[29]

- Surface exposed amino acids (N80, N16, S48) *versus* amino acids buried in the hydrophobic core (L66, I20) have been selected. Only the former will sense changes in protein solvation.

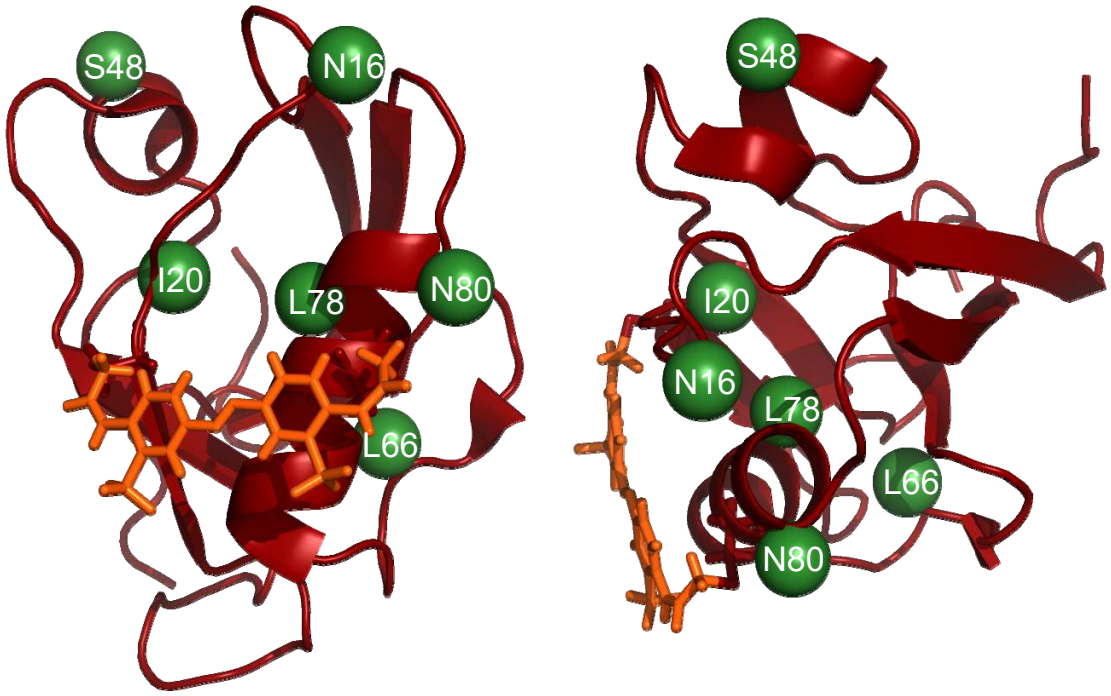

FIG. 1. Photoswitchable PDZ2 domain with the positions of amino acids, which have been mutated to AHA, indicated in green. Only one amino acid has been mutated at a time in the experiment. Left: Front view to the binding site of the protein; right: top view

- Finally, we considered only amino acids of similar size for mutation, and only neutral amino acids in order to avoid shifts of the isoelectric point of the protein.

Fig. 1a,b show all amino acids that have been mutated to AHA (for each mutation, only one amino acid at a time). We use 2D IR spectroscopy instead of FTIR spectroscopy owing to the inherent sensitivity gain of 2D IR, which for the most part originates from its quadratic dependence on the extinction coefficient that significantly reduces the solvent background in a relative sense.[4] Furthermore, since the measurement beams are small, and since we can light-induce the *trans*-to-*cis* transition, extraordinary low amounts of protein sample are needed ($\lesssim$ 1 nmol) in 2D IR difference spectroscopy. These low amounts compensate for the fact that protein preparation is quite tedious.

II. MATERIAL AND METHODS

A. AHA-Labelled, Photoswitchable PDZ2 Domain

To produce protein containing the non-natural amino acid AHA, we have modifed a protocol that has been described before[27] as follows: Starting from the previously used pET30a(+) vector containing two mutations S21C and E76C for the cross-linking of the photoswitch,[29] additional single residues were mutated to methionine for the insertion of AHA by site-directed mutagenesis (QuikChange; Agilent, Santa Clara, CA). A methionine auxotrophic cell strain (E. coli B834(DE3); Novagen, Merck Millipore, Darmstadt, Germany) was used for the protein expression. Cell cultures were grown in LB medium with 30 μg/ml kanamycin at 37°C to an OD600 of 0.8. The LB cultures were centrifuged at 3500 g and 20°C for 20 min and afterwards immediately re-suspended in a minimal medium (SelenoMet Base medium with SelenoMet Nutrient mix from Molecular Dimensions, Newmarket, UK) supplemented with 100 μg/ml AHA (Bapeks, Riga, LV) and 30 μg/ml kanamycin, where they were incubated at 37°C for 30 min in order to use up residual methionine. 1 mM IPTG was added and the protein was expressed at 37°C. AHA is a potentially reactive amino acid and can be modified during protein expression and purifcation. A short expression time of 4 hours was therefore chosen in order to minimize protein modifications, despite a somewhat lower yield. The cell cultures were centrifuged at 3500 g and 4°C for 20 min and then stored at -20°C.

The His-tagged protein was purified using nickel magnetic beads (Biotool.com, Houston, TX, USA) following the recommended protocol. 50 mM Tris buffer, pH 8.5 was used for cell lysis, the protein was denatured with 6 M guanidinium chloride and then refolded on the nickel magnetic beads. Residual nickel, which was bound to the protein, was removed by adding 40 mM EDTA and incubating over night at 4°C. A yield of about 7 mg protein per liter of cell culture was determined using a Bradford assay. SDS-PAGE and mass spectrometry were performed to control the purity of the protein.

As photoswitch, we employed an azobenzene derivative containing two sulfonate ($-SO_3^-$) groups in order to increase its solubility in water.[49] For its cross-linking, a protocol similar to the one described in Ref. 29 was used. However, the reduction of the cysteins, to which the photoswitch binds, had to be performed under milder conditions, since any reducing

agent that is commonly used for that purpose would also reduce the azido group of the AHA, resulting in a primary amine. The reaction conditions had to optimized, so that most of the disulfide bridges were reduced while most of the AHA remained intact. That is, 1 mM TCEP (from a 100 mM TCEP stock at pH 8.5) was added to the protein at a concentration of around 50 to 200 μM in 50 mM Tris buffer, pH 8.5, 500 mM imidazole and 40 mM EDTA. This solution was incubated at room temperature for no longer than 15 min. In principle, the reduction of disulfide bonds could be omitted completely in order to avoid any destruction of AHA, which however, would lower the yield of the cross-linking reaction dramatically.

As in Ref. 29, the reducing agent was subsequently removed by desalting chromatography (HiPrep column, GE Healthcare, 50 mM Tris buffer, pH 8.5), and the protein was cross-linked to the photoswitch under an oxygen free (nitrogen) atmosphere at room temperature for at least 6 hours. Cross-linking was performed in a highly diluted solution in order to minimize the formation of oligomers (10 μM protein to 100 μM photoswitch). The cross-linked protein was purified using anion exchange chromatography (HiTrapQ column, GE Healthcare). The His-tag was removed by digestion with HRV 3C protease, and the cleaved protein was purifed with nickel affinity chromatography (His-Trap HP column, GE Healthcare). The purified protein was concentrated and desalted into 50 mM borate buffer with 150 mM NaCl at pH 8.5. Finally, the protein was lyophilized and dissolved in D_2O. Mass spectra of all mutants considered in this study are shown in Fig. S1 (Supplementary Material), emphasizing the excellent purity of the final labelled and cross-linked protein.

B. Difference 2D IR Spectroscopy

For the difference 2D IR spectroscopy, we used an instrument described before.[20,22] In brief, mid IR pulses were generated in a home-built two stage OPA with a difference mixing stage[50] pumped by a commercial Ti:S amplified laser system (Spitfire, Spectra Physics) running at 5 kHz. The OPA yielded pulses at 4.7 μm and $\approx$3 μJ per pulse with an energy stability better than 0.3% at 500 shots. The 2D-IR instrument used a four wave mixing phase-matching geometry employing a HeNe trace beam to accurately determine the delay times[51] and a polarization-based balanced heterodyne detection.[52] The signal was detected on a 2$\times$32 MCT detector array after dispersing it in a spectrograph with a resolution of

7 cm^{-1}. A photoelastic modulator (PEM) was used to induce a quasi-phase shift on pulses 1 and 2 in order to suppress scattering.[53] The time domain data were collected into 2.11 fs long time bins (defined by the HeNe wavelength) with a maximum scanning time of 3 ps, revealing a spectral resolution of 2.7 cm^{-1} after zero-padding by a factor 2 and subsequent Fourier transformation. Purely absorptive spectra were obtained by alternative scanning of beams 1 and 2 backward in time. The population time was kept constant at 300 fs to minimize non-resonant effects from overlapping excitation pulses.

At the protein concentrations considered in this study (1 mM or below), the AHA signal is buried under the background from the D_2O buffer (essentially the wing of the OD-stretch vibration that is centered at $\sim$2500 cm^{-1}). We therefore measured difference 2D IR spectra, i.e., we first measured a spectrum of the dark adapted protein, in which case the photoswitch is in the *trans* configuration. The sample was then switched into *cis* by illuminating it at 370 nm from a cw-diode laser (CrystaLaser CL-2000) for about 3 min, and a second 2D IR spectrum was measured without changing any of the alignment (but with continuous illumination with the 370 nm laser). The difference of the two spectra was then calculated after phasing them independently, using the phase of the water background also contained in the data as a reference (see Ref. 54 for details). Since the water background is the same in that light-induced difference spectrum, it did not have to be measured independently and a stationary cuvette with only ≈ 1 μl of sample volume was sufficient for these experiments. For the unfolding difference spectrum, on the other hand, L78AHA was resuspended in 6 M guanidinium chloride, deuterated buffer solution at pH 8.5 to ensure complete unfolding. The final spectrum is a double-difference spectrum, i.e. the spectrum in the unfolded state minus that of the corresponding buffer, subtracted from the folded state minus corresponding buffer. To subtract out the buffer contribution, a syringe pump sample delivery system together with a flow cell was used to exchange sample,[20,22] requiring much larger sample volumes of ≈ 100 μl.

C. Molecular Dynamics Simulations

Recently Buchenberg et al. performed a detailed molecular dynamics (MD) study of the structural changes of photoswitchable PDZ2 upon *cis-trans* photoisomerization.[31] Following this work, we carried out MD simulations of photoswitchable PDZ2 including AHA labels

as present in the experiment. To minimize computational time, three labels were considered per simulated system (in contrast to experiment, where only one amino acid was replaced per sample). Selecting label positions such that no AHA group interacts with another one, the first system contained AHA labels at sequence positions 16, 66 and 78, and the second system at positions 20, 48 and 80. Both systems were simulated in the *cis* and *trans* configuration of PDZ2, using Gromacs 4.6.7 with a hybrid GPU-CPU acceleration scheme.[55]

In all simulations, the protein was placed in aqueous solution including 150 mM NaCl. The side chains of all four histidine residues (33, 54, 72, and 87) in all initial structures were chosen to be ϵ-protonated. The protein was described using the Amber99SB*ILDN force field,[56–58] water molecules by the TIP3P model,[59] and ions with the model of Ref. 60. The parameterization procedure using Antechamber[61] and Gaussian09[62] and the resulting force field parameters of the AHA labels are described in the Supplementary Materials. All bonds involving hydrogen atoms were constrained,[63] allowing for a 2 fs time step. Electrostatic interactions were calculated using PME.[64] The minimum cutoff distance for electrostatic and van der Waals interactions was set to 1.2 nm. To couple the system to a heat bath, we used the velocity-rescale algorithm[65] and for pressure coupling the Berendsen algorithm.[66] After energy minimization, the systems were simulated for 100 ns at a pressure of 1 bar and a temperature of 300 K.

Data evaluation was carried out with Gromacs tools.[55] To determine intraprotein polar contacts, we used *g_mindist* to calculate the minimal distances between the $-N_3$ atoms of the AHA residue and all polar atoms which were found within a 1 nm radius of the azido group (with respect to the starting structure). Contact distributions were then obtained by histogramming the MD data with 0.01 nm binning width. We defined a contact to be formed if the minimal distance between a azido group nitrogen atom and a protein nitrogen or oxygen atom is shorter than 0.45 nm.[67] In a similar way, we analyzed contacts between AHA and water as azido group/water oxygen atom distances with a cut-off of 0.45 nm, as well.

D. Calculation of Vibrational Spectra

We used the empirical model of Cho and coworkers[28] to estimate vibrational shifts $\delta\omega$ caused by changes in the electrostatic environment of the AHA labels. By calculating the

electric field $\mathbf{E}_j(t)$ at the nitrogen atoms ($j = 1, 2, 3$) of the azido group for each MD snapshot at time t, we obtain the spectral shift

$$\delta\omega(t) = \sum_j \mathbf{a}_j \mathbf{E}_j(t) \tag{1}$$

with coefficients $\mathbf{a}_j$ given in Ref. 28. Electric fields were computed via a reaction field approach[55,68] using a cut-off radius $r_c = 2.3$ nm. From the frequency trajectory $\delta\omega(t)$ with a time step of 15 ps, the distribution of the vibrational shifts was obtained via a histogram using 50 bins.

As an alternative approach, quantum-mechanical calculations of vibrational spectra of protein side-chain conformers were performed using Gaussian09,[62] following Wolf et al.[69] From the MD simulation, we first determined the snapshot where the $N^{(2)}$-atom of the azido group is closest to one of the two sulfur atoms of the photoswitch sulfonate groups; we chose one structure each for the *trans* and the *cis* configuration, and for I20AHA and L78AHA. Using these structures, we constructed a minimal vacuum model of the AHA label ($-N_3$ group and Cβ atom) and the sulfonate group (including the attached carbon atom), where both carbon atoms were saturated with hydrogen atoms. Keeping the positions of both carbon atoms as well as the distance between $N^{(2)}$-atom and sulfur atoms fixed, the resulting system was initially minimized in energy at the HF/6-31+G* level, followed by a density functional theory-based minimization using B3LYP[70,71] and the 6-31+G* basis set. At the same theoretical level, harmonic frequencies and band intensities were determined by diagonalization of the Hessian matrix. Vibrational frequencies were corrected by the asymmetry factors given in Ref. 72. Atomic charges were calculated via Mulliken population analysis.[73]

III. RESULTS AND DISCUSSION

A. Folding Stability

We have determined the folding stability of the various mutants by CD spectroscopy; the data are shown in Fig. S2 (Supplementary Material) and the results are summarized in Table I. The CD measurements have been performed under the same conditions as the 2D IR experiments, i.e., buffered in D_2O solution. Tentatively, the AHA mutations

destabilize the protein, if at all, only a little bit relative to the photoswichtable PDZ2 domain without AHA, as judged from the midpoint temperatures T_m. The *cis*-state is, overall speaking, somewhat less stable than the *trans*-state (the latter is opposite to what we have reported in Ref. 30, where the CD has however been measured in H_2O and without NaCl). Furthermore, the folding transition is less cooperative in the *cis*-state with a larger width of the folding transitions ΔT. Nevertheless, all mutants considered here are folded to $\gtrsim$98% at 10°C in both their *cis* and their *trans*-states. We performed the 2D IR experiments at that temperature in order to ensure that any difference signal induced by photoswitching is not obscured by partial unfolding.

B. Unfolding 2D IR Difference Spectra

As a reference experiment, Fig. 2 compares the 2D IR spectra of L78AHA in the folded and the unfolded state of the protein. The measurements were performed in the dark, i.e., with the photoswitch in its *trans* configuration. We chose to induce unfolding by a denaturant (6 M guanidinium chloride), rather than by raising the temperature, as the latter causes a dramatic change in the water response and furthermore tends to induce aggregation of the

TABLE I. Unfolding midpoint temperatures T_m and width of the folding transitions ΔT of the different mutations of the photoswitchable PDZ2 domain in its two states, as obtained from CD spectroscopy. To that end, the data have been fit to a function $1/(1+\exp((T-T_m)/\Delta T))$ after subtraction of the background and normalisation.

Mutant	***trans***		***cis***	
	T_m/°C	ΔT/°C	T_m/°C	ΔT/°C
no AHA	49.5±1	3.7±1	46.0±2	6.3±2
N16AHA	48.0±1	5.4±1	45.5±2	8.0±2
I20AHA	43.0±1	5.2±1	36.5±4	7.9±2
S48AHA	49.5±1	3.9±1	51.0±1	3.8±1
L66AHA	44.5±1	4.2±1	43.5±1	5.9±1
L78AHA	43.5±1	4.4±1	38.5±2	7.4±2
N80AHA	47.0±1	4.5±1	49.0±3	6.0±3

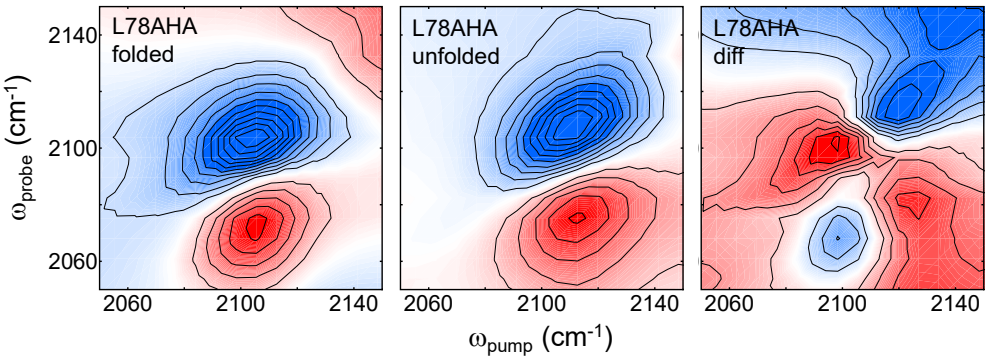

FIG. 2. Purely absorptive 2D IR spectra of L78AHA in the folded (left panel) and the unfolded state (middle panel), the latter induced by adding 6 M guanidinium chloride. The right panel shows the difference (unfolded minus folded) of both spectra. To that end, the spectra of the folded and unfolded protein have been scaled to the bleach signal, since they have been measured at slightly different concentrations, and have subsequently been subtracted to reveal the difference spectrum. For the plotting, the difference spectrum has been multiplied by a factor 2 so that all spectra share the same number of contour lines. Blue colors depict negative signals (i.e., bleach and stimulated emission in the purely absorptive 2D IR spectra) and red colors positive signals (excited state absorption).

protein and hence scattering in the 2D IR signal. In each case, a 2D IR spectrum of the corresponding buffer has been measured as well under identical conditions, and has been subtracted, as shown in Refs. 4, 20, and 22. In both states of the protein, the 2D IR spectra show the usual 0-1 peak depicted in blue together with the 1-2 peak depicted in red (i.e., with opposite sign), which is shifted along the probe-frequency axis due to the anharmonicity of the AHA vibration. By the tilt of the 2D IR lineshapes, a modest amount of inhomogeneity is detected, which does not differ very much in the two states of the protein.

The most prominent change upon unfolding is a blue-shift of the AHA label by $\approx$7 cm^{-1}, which is a bit smaller than for previous observations.[17] That is, upon unfolding, the AHA label becomes fully solvated and hence the number of hydrogen bonds to water molecules increases, as well as their flexibility allowing for hydrogen bonding at a more optimal angle. Cho and coworkers have shown in Ref. 18 that both effects cause a blue shift of the vibrational transitions. In turn, the frequency shift also reveals that the AHA label of this particular mutant is solvent-exposed to only a minor extent in the folded state of the protein. Position

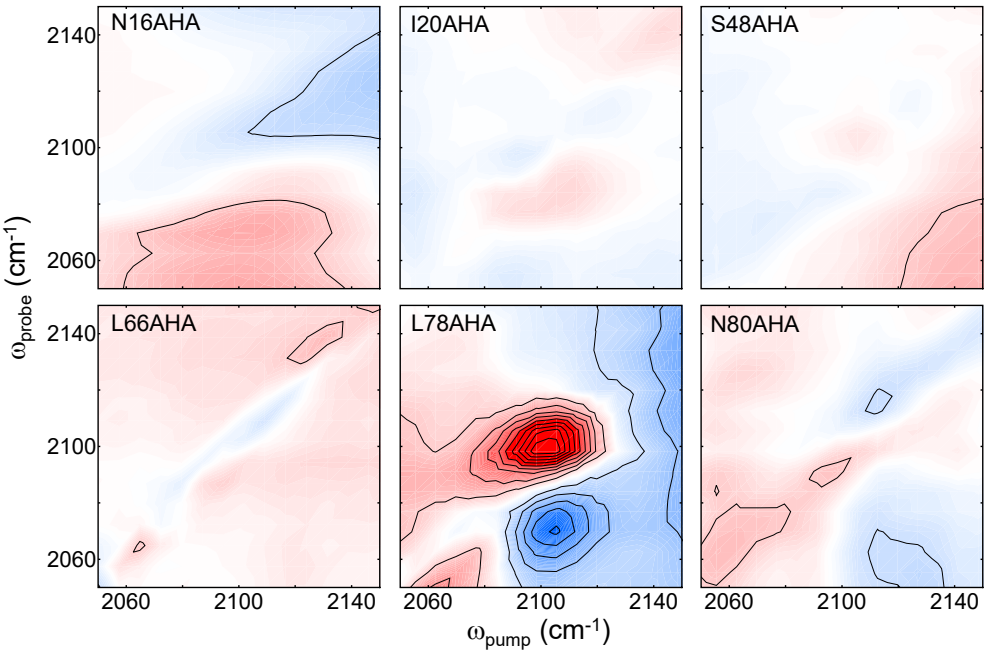

FIG. 3. Purely absorptive 2D IR difference spectra (*cis* minus *trans*) of all mutants considered in this study, induced by photoswitching the azobenzene moiety from *trans* to *cis* with the help of a cw-laser diode. All signals were normalized by concentration (which varied between 0.6 mM and 1.1 mM) and to the peak signal of L78AHA. Blue colors depict negative signals and red colors positive signals.

L78AHA is situated inside the the binding pocket (see Fig. 1), where the access of the solvent is limited, possibly shielded by the azobenzene photoswitch (see below).

C. Photoswitching 2D IR Difference Spectra

With that information in mind, we turn to the 2D IR difference spectroscopy induced by photoswitching the azobenzene moiety from *trans* to *cis* with the help of a cw-laser diode. Fig. 3 shows the spectra of all mutants that have been investigated. Surprisingly, only one of the considered mutants (L78AHA) reveals an evaluable signal, while all others show no clear signal apart from some modifications of the water background and/or small remaining scattering (the latter appears as spurious signals along the diagonal, see e.g. the 2D IR difference spectra of L66AHA or N80AHA). These two effects currently limit our sensitivity, not signal-to-noise *per se*. It should however be stressed that we know beyond any doubt

that the AHA label is present also in those mutants, for which no difference signal could be detected. For example, we see its absorption band in the individual dark-adapted (*trans*) 2D IR spectra, i.e., before taking the difference with the corresponding *cis* 2D IR spectra (however, sitting on a large water background, see Fig. S3, Supplementary Material). Also mass spectrometry (Fig. S1, Supplementary Material) confirms the existence of an azido group in all mutants.

Nonetheless, the response of L78AHA, and the comparison to the unfolding difference spectrum from Fig. 2, is quite revealing. The 2D IR difference spectrum induced by photoswitching (Fig. 3) is quite comparable to the 2D IR spectrum of the folded state (Fig. 2, left panel), where the frequency position and 2D line shape is concerned, but the sign (encoded by the colors) is inverted and the intensity is about a factor 5 smaller. Furthermore, the photoswitch induced difference spectrum is very different from the unfolding induced difference spectrum (Fig. 2, right panel), the latter of which resulting from the frequency shift of the AHA transition. That is, the effect of photoswitching on the AHA label is mostly a reduction of the vibrational transition dipole in the *cis*-state without affecting the vibrational frequency very much. This in turn also evidences that the difference spectrum induced by photoswitching is not the result of the slightly reduced stability of the protein with the photoswitch in the *cis* state, which according to CD spectroscopy (Supplementary Material, Fig. S2) might cause ≈2% of unfolding.

To the best of our knowledge, this effect has not been described so far. That is, while the frequency of the AHA label is considered to be a measure of the amount of solvation,[16–22] the intensity stays essentially the same, which is indeed what is observed when unfolding the protein (Fig. 2). It is conceivable that when the label enters a more heterogenous environment, the absorption becomes wider at the expense of the peak intensity such that the integrated intensity, and hence the transition dipole, stays the same. We tentatively exclude that effect here, since it would cause wings of opposite sign on both sides of the peak in the difference spectrum that are not observed, even when considering the present signal-to-noise level. We also carefully checked the possibility that the loss of intensity reflects a loss of AHA label due to a reduction of the azido group, for example. To that end, we first measured mass spectra before and after laser illumination (see Fig. S4, Supplementary Material), showing that no chemical modification is occurring, such as the loss of a N_2 molecule. Second, we measured FTIR difference spectra switching forth and back, evidencing that the transition is

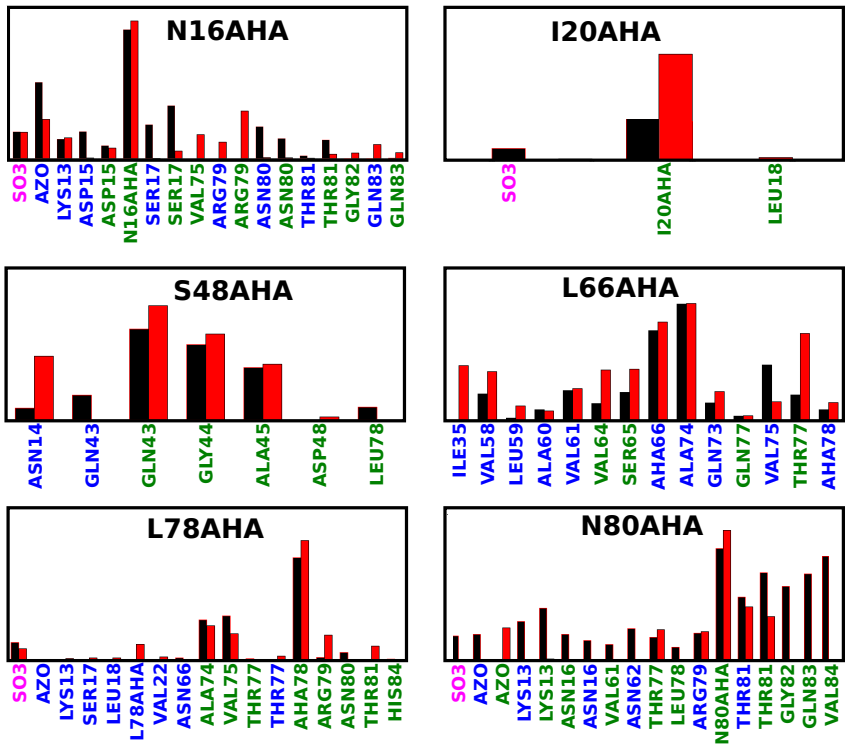

FIG. 4. Histograms of polar contacts between considered AHA labels and PDZ2 protein in *cis* (black) and *trans* (red) state. Green and blue labels denote backbone and side-chain contacts, respectively, and magenta labels indicates contacts with the sulfonate groups of the photoswitch.

indeed reversible and that the AHA band regains its intensity upon *cis-trans* back-switching (see Fig. S5, Supplementary Material).

D. Spectral Simulations

To get insights into the molecular mechanism giving rise to this spectroscopic response, we performed spectral simulations based on all-atom MD simulations. Recent quantum-chemical calculations of Cho and coworkers[18] have shown that the spectroscopic signatures of the azido stretch mode of AHA mainly reflect the local electrostatic environment of the azido group. To result in an observable IR difference spectrum of PDZ2, this electrostatic field needs to differ in the *trans* and the *cis* states. Since the main contributions to the local electrostatic environment arise from contacts with nearby polar residues and water molecules, we first employ MD simulations to study possible changes of these contacts caused

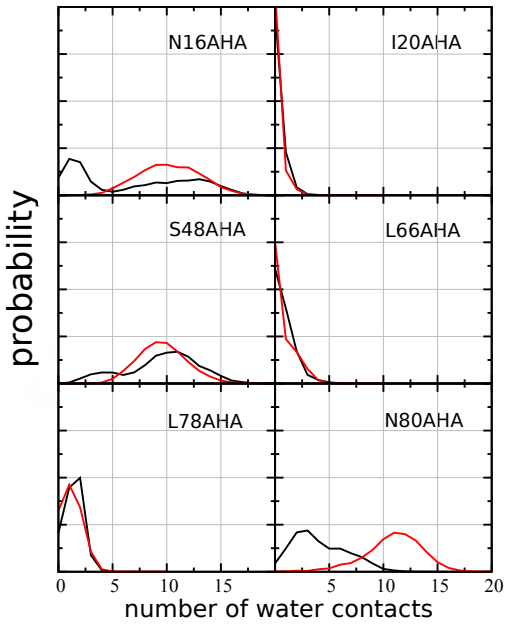

FIG. 5. Distribution of the number of water contacts of the AHA labels, with the protein being in *trans* (red) and *cis* (black) state.

by the *trans-cis* isomerization.

Let us begin with the contacts between polar protein residues and the azido groups. Fig. 4 reveals that the number of such intraprotein contacts and their changes upon *trans-cis* photoisomerization appear quite complex. Roughly speaking, we find three labels (N16AHA, L66AHA, N80AHA) with a large number, two (S48AHA, L78AHA) with a medium number, and one (I20AHA) with a small number of intraprotein contacts. Notably, we see that labels N16AHA, I20AHA and N80AHA show significant contact changes between *trans* and *cis* states, while the label L78AHA shows only minor variations. Fig. 5 displays the distribution of water contacts during the MD simulation. Three AHA labels (N16AHA, S48AHA, N80AHA) are found to be strongly hydrated, two (I20AHA, L66AHA) are hardly hydrated, and label L78AHA, for which a difference signal could be observed experimentally, may be characterized as moderately hydrated. Interestingly, only the strongly hydrated labels show significant differences in the number of water contacts between *trans* and *cis* states. In particular, we find that the decrease in the number of water contacts of N16AHA and N80AHA upon *trans-cis* photoisomerization is compensated by an increase of protein contacts.

As the examination of the changes of contacts does not provide a clear explanation of the

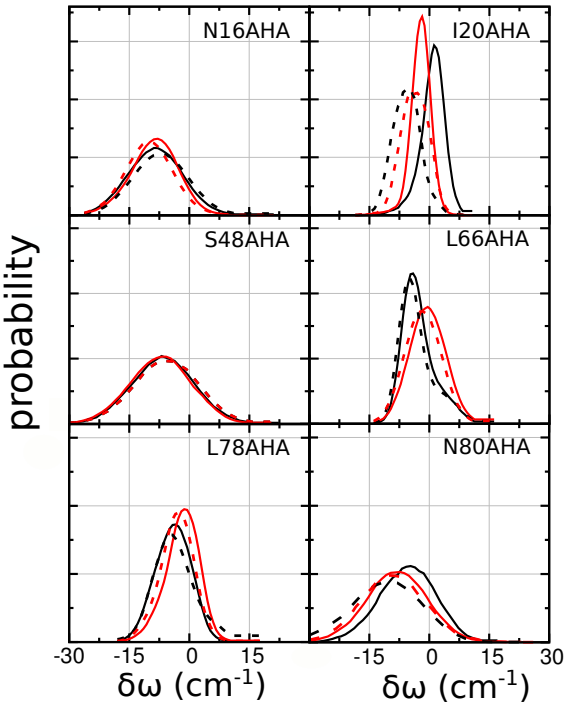

FIG. 6. Vibrational frequency shifts (relative to the gas-phase vibration) of the azido stretch mode of the AHA labels in the *trans* (red) and *cis* (black) states. Results are obtained from the electrostatic model (Eq. (1)) with (full lines) and without (dashed lines) inclusion of the sulfonate groups of the photoswitch.

experimental findings, we next study to what extent the contact changes discussed above are reflected in spectral changes of the azido stretch mode of the corresponding AHA label. To this end, Fig. 6 displays the distribution of vibrational frequency shifts $\delta\omega(t)$ upon *trans-cis* photoisomerization, as obtained from the electrostatic model in Eq. (1). In the case of the strongly hydrated labels (N16AHA, S48AHA, N80AHA), the calculations predict relatively broad ($\sim \pm 10\,\mathrm{cm}^{-1}$) and red-shifted (by $\sim 10\,\mathrm{cm}^{-1}$) frequency distributions. The weakly to hardly hydrated labels (I20AHA, L66AHA, L78AHA), on the other hand, exhibit a smaller distribution width ($\sim \pm 5\,\mathrm{cm}^{-1}$) and also smaller frequency shifts. This different width of the frequency distributions of hydrated vs. not hydrated labels is in nice agreement with the experimental results of Taskent-Sezgin et al.,[17] who found line widths of $\sim \pm 5$ and $10\,\mathrm{cm}^{-1}$ for AHA labels in the folded and unfolded (i.e., water exposed) state of a protein, respectively. On the other hand, we note that the overall redshift predicted by the model is in variance with the common expectation that solvation rather causes a blue shift (see, e.g.,

Fig. 2 as well as Refs. 1, 17, 20–22). As discussed in Ref. 28 [Fig. 6], this effect is caused by our neglect of the polarizability of the azido group.

Upon *trans-cis* photoisomerization, the strongly hydrated labels show no or only minor spectral changes. This is clearly expected for S48AHA, where both protein and water contacts remain more or less unchanged, but comes a bit as a surprise for N16AHA and N80AHA, where both protein and water contacts change significantly. We conclude that the highly mobile water molecules around these labels may effectively screen or counter the electrostatic interactions of the protein, which hampers a clear spectroscopic response. The frequency distribution of L78AHA hardly changes between *trans* and *cis* states, which is in line with the absence of major protein or water contact changes for this label. On the other hand, the spectral simulations would predict a significant blue shift of I20AHA and L66AHA when changing from *trans* to *cis*, resulting from the changes of protein contacts, which however is not observed experimentally.

To sum up the results up to this point, our MD simulations combined with the electrostatic model by Cho and coworkers[28] would predict spectral changes for I20AHA and L66AHA, while in experiment L78AHA is the only label with an observable spectral response upon *trans-cis* photoisomerization. Of course, one may question the accuracy of the structural prediction of the employed MD force field (neglecting, e.g., the polarizability of the azido group) or the assumptions underlying the electrostatic model (neglecting, e.g., the dependence on dispersive interactions or the fact that the model of Cho and coworkers[28] has been parameterized based on QM calculations with water clusters around an azido group only, while intraprotein contact to polar residue play a significant role here as well). Moreover, the electrostatic model would describe frequency shifts only, which is not what is observed experimentally. That is, the experimental 2D IR difference spectrum upon *trans-cis* photoisomerization is dominated by a change in the intensity of the vibration of L78AHA, and not its frequency.

Being a 1,3-dipole, the azido group is strongly polarizable, and it is for example well known that azido groups in different molecules have strongly varying transition dipoles.[5] Hence, it is conceivable that even weak electronic interactions with other parts of the protein, involving for example a charge transfer similar to the situation in a hydrogen bond or at the onset of a nucleophilic attack, may strongly affect the electronic density of the azido group and thereby change the transition dipole of its vibration. The prime candidates

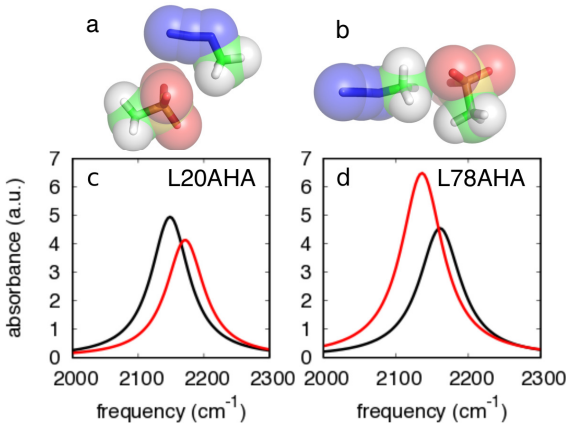

FIG. 7. Quantum-chemical calculations for a minimal model of the AHA label ($-N_3$ group and Cβ atom) and the sulfonate group of the photoswitch, indicating the van der Waals radii of the atoms by colored spheres. Panels (a) and (b) show energy-minimized structures of L78AHA in *cis* with contact and *trans* without contact, respectively, of the azido and the sulphonate groups. I20AHA exhibited similar structures, with a contact in *trans* and without contact in *cis* (not shown). Using these structures, vibrational spectra of the azido stretch mode were calculated for (c) I20AHA and (d) L78AHA. Black and red lines correspond to the *cis* and *trans* state of the photoswitch, respectively.

for such an electronic interaction are the two sulphonate groups of the photoswitch, which have been introduced to increase the solubility of the azobenzene moiety.[49] Performing electrostatic calculations in the absence of these sulfonate groups (dashed lines in Fig. 6), the frequency distributions of I20AHA and L78AHA reveal a significant red-shift, emphasizing the importance of the sulfonate groups. Moreover, the red-shifts are clearly different for *trans* and *cis* states. The strongly hydrated labels N16AHA and N80AHA, on the other hand, show only minor spectral changes when sulfonate groups are excluded in the electrostatic calculations. Although these labels form contacts with the sulfonate groups (Fig. 4), the strong electrostatic screening due to solvent water appears to prevent clear spectral changes.

In our MD simulations, such contacts don't appear often (cf. Fig. 4), owing to the missing stabilizing electronic interaction in the force field description. To investigate if such direct contacts between azido and sulfonate groups can lead to a charge transfer and the experimentally observed absorbance changes, we extracted the structure with the closest distance between I20AHA/L78AHA and an neighboring sulfonate group from MD simulations of each

cis and *trans* states. Showing the energy-minimized structures of these states, Figs. 7a and b reveal that L78AHA indeed forms a close contact with the sulfonate group, which mediates an electronic interaction. Intriguingly, this contact only exists in the *cis* configuration of the photoswitch, but not in the *trans* configuration. Likewise, an energy-minimized structure of I20AHA (not shown) exhibits a close contact associated with an electronic interaction in the *trans* configuration, that does not exists in the *cis* configuration.

Using these structures, we calculated harmonic frequencies and band intensities of the azido stretch mode (see Methods). Figure 7c and d show the resulting vibrational spectra of the azido stretch mode of I20AHA and L78AHA in the *cis* and *trans* states of the photoswitch. In either case, a close contact between the azido and the sulfonate groups results in a decrease of the band intensity of the AHA vibration due to a charge transfer to the azido group that reduces the transition dipole. As can be seen in Table II, the charge on all nitrogen atoms changes by up to $\pm 0.23\,e$, indicating that the charges on the azido group are indeed very mobile due to electronic effects. A polarizable force field is the least that would be needed to describe that effect self-consistently in a MD simulation. The effect on intensity is stronger for L78AHA than for I20AHA, in qualitative agreement with experiment. It should however be mentioned that in addition to the intensity change, the quantum chemistry calculations would also predict a frequency shift of ~ 25 cm^{-1}, which is not observed in experiment. Possibly, the missing protein environment and solvation in the

TABLE II. Mulliken charges[73] (in units of e) of the AHA azido nitrogen atoms in different quantum chemical vacuum models. Cont./no cont. refer to the presence/absence of a contact with the neighboring sulfonate group. $N^{(3)}$: nitrogen attached to AHA side chain; $N^{(2)}$: internal nitrogen atom; $N^{(1)}$: terminal nitrogen atom.

nitrogen	**I20AHA**		**L78AHA**	
atom	***cis***	***trans***	***cis***	***trans***
	no cont.	**cont.**	**cont.**	**no cont.**
$N^{(3)}$	-0.45	-0.33	-0.52	-0.50
$N^{(2)}$	1.02	1.21	1.08	0.89
$N^{(1)}$	-0.71	-0.94	-0.67	-0.54

quantum chemistry calculations might be responsible for that effect. The results nevertheless suggest that weak electronic interactions may indeed change the intensity of the AHA vibration, enabling a new application for that vibrational label.

IV. CONCLUSION

The AHA vibration is an attractive label to study protein structure and dynamics with the help of IR and 2D IR spectroscopy, since it can be incorporated almost anywhere in a protein by a methionine auxotrophic protein expression strategy,[26,27] since its transition dipole is reasonably large for 2D IR measurements in the sub-mM regime,[4,22] and since it is a sensitive probe of its solvation environment.[1,17–22,28] However, in order to demonstrate the last aspect, rather dramatic changes have been applied to the label so far. For example, a protein has been unfolded, which fully exposes an AHA label that normally is situated in the hydrophobic core of the protein to water,[17] or a peptide ligand with an AHA label has been dissociated from a protein,[20,22] which has about the same impact on the label as unfolding. Employing a combined experimental-computational approach, we set out in the present work to explore the capability of the AHA label to also sense much smaller changes in the structure and solvation of a mid-sized protein. That is, rather than unfolding of a protein, we change the structure of a PDZ2 domain in a very modest way ($\lesssim 1$ Å) with the help of a photoswitch that is covalently linked to it, thereby mimicking the conformational transition upon ligand binding.[29,31,32]

To that end, we first had to develop a protocol for the post-translational synthesis of the cross-linked PDZ2 domain containing AHA labels. That is, both the cysteins needed for the linking of the azobenzene photoswitch as well as the azido groups of AHA are chemically very reactive groups. For AHA, this reactivity has been used successfully for click chemistry reactions,[74] however, any modification of this unnatural amino acid had to be avoided in our case. Mainly, the reduction of disulfide bridges had to be optimized, such that AHA would not be reduced at the same time into a primary amine.

We have explored six mutations, distributing the AHA label at various positions of the protein that differ significantly in their properties (Fig. 1), e.g., inside the hydrophobic core *versus* surface exposed, or in the flexible loops *versus* in more rigid secondary structure motives. We find that because of the fact that the label is very small and of medium

polarity, it can replace both polar and apolar amino acids without affecting the stability of the protein too much (Table I). In that sense, it is indeed a versatile label.

Somewhat surprisingly, however, we observe an evaluable difference 2D IR signal upon photoswitching only for one mutation, L78AHA (we nevertheless chose to show all results in Fig. 3, including the negative ones, since the purpose of this survey has been to learn what can be sensed with the AHA label, and what its limitations are). The very distinct difference signal of only the one label L78AHA comes as a surprise, since I20AHA and N80AHA are equally close to perturbation introduced by the photoswitch. Naturally, one would assume that the size of the effect correlates with the distance to the perturbation; yet, with our current experimental sensitivity we cannot detect any response for I20AHA and N80AHA. It also comes as a surprise, since the MD simulations would in fact predict significant changes of local contacts to both water molecules and protein side chains, even for labels that are quite far away from the photoswitch, such as N16AHA or L66AHA (see Fig. 4 and 5).

The distinct response of L78AHA, in turn, suggests that it results from a very specific interaction that should be robustly reproduced by a MD simulation, even given the unavoidable imperfectness of any MD force field that might describe some structural details in not quite the correct way. We therefore first employed classical MD simulations, calculating local contacts of the various AHA labels with its surrounding (Figs. 4 and 5) as well as electric field induced frequency shifts along the line of a model put forward by Cho and coworkers (Fig. 6).[28] The simulation revealed that the strongly hydrated labels show no or only minor spectral changes, even if both protein and water contacts change significantly (as is the case for N16AHA and N80AHA). This suggests that this is the result of a mutual cancellation of the contributions from water and the protein. That is, the highly mobile water molecules around these labels effectively screen or counter the electrostatic interactions of the protein.

On the other hand, the calculations revealed nothing with respect to which L78AHA would stick out. In the contrary, they predict a frequency shift for I20AHA and L66AHA that are of the same order as in the unfolding experiment of Fig. 2 or what has been observed in Ref. 22 for ligand unbinding, and thus should be measurable with our current sensitivity. One possible explanation for that discrepancy might be the fact that the electrostatic model of Cho and coworkers[28] neglects polarizability and has been parameterized based on quantum chemical calculations focusing on hydrogen bonding in water clusters around a solvated azido

group only, while L66AHA and I20AHA are basically not solvated (Fig. 5) and the electric field in Eq. (1) originates mostly from intra-peptide contact with polar side-groups.

In order to explain the distinct response of L78AHA, which actually reflects a change of intensity of the AHA vibration rather than its frequency, we speculate here that it originates from an electronic interaction between the AHA label and the sulfonate groups of the azobenzene-moiety. As a proof of principle, preliminary gas-phase quantum chemistry calculations, using structures derived from the classical MD simulation, give evidence that this might indeed be the case (Fig. 7). We must concede that we did not do these calculations on a sample of possible contact structures, that the agreement with experiment is rather modest, and that a polarizable force field or QM/MM simulations would be needed to verify that mechanism. As the interaction of the azido group with the sulfonate group is related to a weak chemical bond, the effect might be amplified in a QM/MM simulation, thus increasing the stability and occurrence of contact structures. The same seems to happen also upon hydrogen bonding to water, as evidenced by the observation of Cho and coworkers[18,28] that QM/MM simulations are necessary to correctly descibe the water structure around the azido group, which is a prerequisite for predicting a blue shift upon solvation.

Despite the preliminary character, the current results nevertheless show that the intensity of the AHA vibration carries information about its surrounding that is complementary to the frequency position. This effect has not been described in literature to the best of our knowledge, and needs to be taken into account when analyzing difference spectra from IR labels that can undergo electronic interactions with neighboring amino acids, such as azido and cyano groups. In a broader sense, it reminds one that in difference spectroscopy, band disappearances do not necessarily need to be an effect of a vanishing state population, but can as well stem from effects altering the transition dipole moment of the reporting label. In conclusion, we have found a new and unexpected mode of spectral response of an AHA label incorporated into a protein. This response stems from an electronic instead of an electrostatic interaction of the AHA azido group with the protein/water surrounding, and opens up new applications for the usage of artificial probes in biospectroscopy.

Supporting Information: Details of the force field parametrisation of the AHA group, as well as mass spectra determining the purity of the samples, temperature-dependent CD spectra determining their stability, 2D IR spectra of the dark-adapted (*trans*) state, and

FTIR difference spectra are given in Supporting Information. This information is available free of charge via the Internet at http://pubs.acs.org

Acknowledgement: We thank Ben Schuler and his group for their continuous and tremendous help with the protein chemistry, Brankica Janković for helpful discussion regarding the sample preparation, Steven Waldauer for his idea to use magnetic beads for a faster protein purification, and the Functional Genomics Center Zurich, especially Serge Chesnov, for help with the mass spectrometry. The work has been supported in part by a European Research Council (ERC) Advanced Investigator Grant (DYNALLO), by the Swiss National Science Foundation (SNF) through the NCCR MUST and Grant 200021_165789/1, as well as by the Deutsche Forschungsgemeinschaft through Grant STO 247/10-1. Computational resources were provided by the bwForCluster BinAC (RV bw16I016) and the Black Forest Grid Initiative.

References:

[1] Waegele, M. M.; Culik, R. M.; Gai, F. Site-Specific Spectroscopic Reporters of the Local Electric Field, Hydration, Structure, and Dynamics of Biomolecules., *J. Phys. Chem. Lett.* **2011**, *2*, 2598–2609.

[2] Adhikary, R.; Zimmermann, J.; Dawson, P. E.; Romesberg, F. E. IR Probes of Protein Microenvironments: Utility and Potential for Perturbation, *ChemPhysChem* **2014**, *5*, 849–853.

[3] Kim, H.; Cho, M. Infrared Probes for Studying the Structure and Dynamics of Biomolecules, *Chem. Rev.* **2013**, *113*, 5817–5847.

[4] Koziol, K. L.; Johnson, P. J. M.; Stucki-Buchli, B.; Waldauer, S. A.; Hamm, P. Fast Infrared Spectroscopy of Protein Dnamics: Advancing Sensitivity and Selectivity, *Curr. Opin. Struct. Biol.* **2015**, *34*, 1–6.

[5] Ma, J.; Pazos, I. M.; Zhang, W.; Culik, R. M.; Gai, F. Site-Specific Infrared Probes of Proteins, *Annu. Rev. Phys. Chem.* **2015**, *66*, 357–377.

[6] Koziński, M.; Garrett-Roe, S.; Hamm, P. 2D-IR Spectroscopy of the Sulfhydryl Band of Cysteines in the Hydrophobic Core of Proteins, *J. Phys. Chem. B* **2008**, *112*, 7645–7650.

[7] Naraharisetty, S. R. G.; Kasyanenko, V. M.; Zimmermann, J.; Thielges, M.; Romesberg, F. E.; Rubtsov, I. V. C-D Modes of Deuterated Side Chain of Leucine as Structural Reporters via Dual-frequency Two-dimensional Infrared Spectroscopy, *J. Phys. Chem. B* **2009**, *113*, 4940–4946.

[8] Schade, M.; Moretto, A.; Crisma, M.; Toniolo, C.; Hamm, P. Vibrational Energy Transport in Peptide Helices after Excitation of C-D Modes in Leu-D10, *J. Phys. Chem. B* **2009**, *113*, 13393–13397.

[9] Zimmermann, J.; Thielges, M. C.; Yu, W.; Dawson, P. E.; Romesberg, F. E. Carbon-Deuterium Bonds as Site-Specific and Nonperturbative Probes for Time-Resolved Studies of Protein Dynamics and Folding, *J. Phys. Chem. Lett.* **2011**, *2*, 412–416.

[10] Anfinrud, P. A.; Han, C.; Hochstrasser, R. M. Direct Observations of Ligand Dynamics in Hemoglobin by Subpicosecond Infrared-Spectroscopy, *Proc. Natl. Acad. Sci. USA* **1989**, *86*, 8387–8391.

[11] Lim, M.; Jackson, T. A.; Anfinrud, P. A. Mid-Infrared Vibrational Spectrum of CO after Photodissociation from Haem: Evidence for a Ligand Docking Site in the Haem Pocket of Haemoglobin and Myoglobin, *J. Chem. Phys.* **1995**, *102*, 4355–4366.

[12] Thielges, M. C.; Fayer, M. D. Protein Dynamics Studied with Ultrafast Two-Dimensional Infrared Vibrational Echo Spectroscopy, *Acc. Chem. Res.* **2012**, *45*, 1866–1874.

[13] Woys, A. M.; Mukherjee, S. S.; Skoff, D. R.; Moran, S. D.; Zanni, M. T. A Strongly Absorbing Class of Non-Natural Labels for Probing Protein Electrostatics and Solvation with FTIR and 2D IR Spectroscopies, *J. Phys. Chem. B* **2013**, *117*, 5009–5018.

[14] Peran, I.; Oudenhoven, T.; Woys, A. M.; Watson, M. D.; Zhang, T. O.; Carrico, I.; Zanni, M. T.; Raleigh, D. P. General Strategy for the Bioorthogonal Incorporation of Strongly Absorbing, Solvation-Sensitive Infrared Probes into Proteins, *J. Phys. Chem. B* **2014**, *118*, 7946–7953.

[15] King, J. T.; Arthur, E. J.; Brooks, C. L.; Kubarych, K. J. Crowding Induced Collective Hydration of Biological Macromolecules Over Extended Distance, *J. Am. Chem. Soc* **2014**, *136*, 188–194.

[16] Oh, K.-I.; Lee, J.-H.; Joo, C.; Han, H.; Cho, M. β-Azidoalanine as an IR Probe: Application to Amyloid Aβ(16-22) Aggregation, *J. Phys. Chem. B* **2008**, *112*, 10352–10357.

[17] Taskent-Sezgin, H.; Chung, J.; Banerjee, P. S.; Nagarajan, S.; Dyer, R. B.; Carrico, I.; Raleigh, D. P. Azidohomoalanine: A Conformationally Sensitive IR Probe of Protein Folding Protein

Structure and Electrostatics, *Angew. Chemie - Int. Ed.* **2010**, *49*, 7473–7475.

[18] Choi, J. H.; Raleigh, D.; Cho, M. Azido Homoalanine is a Useful Infrared Probe for Monitoring Local Electrostatistics and Side-Chain Solvation in Proteins, *J. Phys. Chem. Lett.* **2011**, *2*, 2158–2162.

[19] Thielges, M. C.; Axup, J. Y.; Wong, D.; Lee, H. S.; Chung, J. K.; Schultz, P. G.; Fayer, M. D. Two-Dimensional IR Spectroscopy of Protein Dynamics Using Two Vibrational Labels: A Site-Specific Genetically Encoded Unnatural Amino Acid and an Active Site Ligand, *J. Phys. Chem. B* **2011**, *115*, 11294–11304.

[20] Bloem, R.; Koziol, K.; Waldauer, S.; Buchli, B.; Walser, R.; Samatanga, B.; Jelesarov, I.; Hamm, P. Ligand Binding Studied by 2D IR Spectroscopy Using the Azidohomoalanine Label, *J. Phys. Chem. B* **2012**, *116*, 13705–13712.

[21] Wolfshorndl, M. P.; Baskin, R.; Dhawan, I.; Londergan, C. H. Covalently Bound Azido Groups are Very Specific Water Sensors, Even in Hydrogen-Bonding Environments, *J. Phys. Chem. B* **2012**, *116*, 1172–1179.

[22] Johnson, P. J. M.; Koziol, K. L.; Hamm, P. Quantifying Biomolecular Recognition with Site-Specific 2D Infrared Probes, *J. Phys. Chem. Lett.* **2017**, *8*, 2280–2284.

[23] Bagchi, S.; Boxer, S. G.; Fayer, M. D. Ribonuclease S Dynamics Measured Using a Nitrile Label with 2D IR Vibrational Echo Spectroscopy, *J. Phys. Chem. B* **2012**, *116*, 4034–4042.

[24] Zimmermann, J.; Thielges, M. C.; Seo, Y. J.; Dawson, P. E.; Romesberg, F. E. Cyano Groups as Probes of Protein Microenvironments and Dynamics, *Angew. Chem. Int. Ed.* **2011**, *50*, 8333–8337.

[25] van Wilderen, L. J. G. W.; Kern-Michler, D.; Müller-Werkmeister, H. M.; Bredenbeck, J. Vibrational Dynamics and Solvatochromism of the Label SCN in Various Solvents and Hemoglobin by Time Dependent IR and 2D-IR Spectroscopy, *Phys. Chem. Chem. Phys.* **2014**, *16*, 19643–19653.

[26] Kiick, K. L.; Saxon, E.; Tirrell, D. A.; Bertozzi, C. R. Incorporation of Azides into Recombinant Proteins for Chemoselective Modification by the Staudinger Ligation, *Proc. Natl. Acad. Sci. USA* **2002**, *99*, 19.

[27] Simon, M.; Zangemeister-Wittke, U.; Plückthun, A. Facile Double-Functionalization of Designed Ankyrin Repeat Proteins Using Click and Thiol Chemistries., *Bioconjugate Chem.* **2012**, *23*, 279–286.

[28] Choi, J.-H.; Oh, K.-I.; Cho, M. Azido-Derivatized Compounds as IR Probes of Local Electro-

static Environment: Theoretical Studies, *J. Chem. Phys.* **2008**, *129*, 174512.

[29] Buchli, B.; Waldauer, S. A.; Walser, R.; Donten, M. L.; Pfister, R.; Blöchliger, N.; Steiner, S.; Caflisch, A.; Zerbe, O.; Hamm, P. Kinetic Response of a Photoperturbed Allosteric Protein., *Proc. Natl. Acad. Sci. USA* **2013**, *110*, 11725–11730.

[30] Waldauer, S. A.; Stucki-Buchli, B.; Frey, L.; Hamm, P. Effect of Viscogens on the Kinetic Response of a Photoperturbed Allosteric Protein, *J. Chem. Phys.* **2014**, *141*, 22D514.

[31] Buchenberg, S.; Knecht, V.; Walser, R.; Hamm, P.; Stock, G. Long-Range Conformational Transition of a Photoswitchable Allosteric Protein: A Molecular Dynamics Simulation Study, *J. Phys. Chem. B* **2014**, *118*, 13468–13476.

[32] Buchenberg, S.; Sittel, F.; Stock, G. Time-Resolved Observation of Protein Allosteric Communication, *Proc. Natl. Acad. Sci.* **2017**, *114*, E6804–E6811.

[33] Kozlov, G.; Gehring, K.; Ekiel, I. Solution Structure of the PDZ2 Domain from Human Phosphatase hPTP1E and its Interactions with C-Terminal Peptides from the Fas Receptors, *Biochemistry* **2000**, *39*, 2572–2580.

[34] Kozlov, G.; Banville, D.; Gehring, K.; Ekiel, I. Solution Structure of the PDZ2 Domain from Cytosolic Human Phosphatase hPTP1E Complexed with a Peptide Reveals Contribution of the Beta 2-Beta 3 Loop to PDZ Domain-Ligand Interactions, *J. Mol. Biol.* **2002**, *320*, 813–820.

[35] Zhang, J.; Sapienza, P. J.; Ke, H.; Chang, A.; Hengel, S. R.; Wang, H.; Phillipsand, G. N.; Lee, A. L. Crystallographic and Nuclear Magnetic Resonance Evaluation of the Impact of Peptide Binding to the Second PDZ Domain of Protein Tyrosine Phosphatase 1E, *Biochemistry* **2010**, *49*, 9280–9291.

[36] Fuentes, E. J.; Der, C. J.; Lee, A. L. Ligand-Dependent Dynamics and Intramolecular Signalling in a PDZ Domain, *J. Mol. Biol.* **2004**, *335*, 1105–1115.

[37] Fuentes, E. J.; Gilmore, S. A.; Mauldin, R. V.; Lee, A. L. Evaluation of Energetic and Dynamic Coupling Networks in a PDZ Domain Protein., *J. Mol. Biol.* **2006**, *364*, 337–351.

[38] Gianni, S.; Walma, T.; Arcovito, A.; Calosci, N.; Bellelli, A.; Engström, A.; Travaglini-Allocatelli, C.; Brunori, M.; Jemth, P.; Vuister, G. W. Demonstration of Long-Range Interactions in a PDZ Domain by NMR, Kinetics, and Protein Engineering., *Structure* **2006**, *14*, 1801–1809.

[39] Ota, N.; Agard, D. A. Intramolecular Signaling Pathways Revealed by Molecular Anisotropic Thermal Diffusion, *J. Mol. Biol.* **2005**, *351*, 345–354.

[40] De Los Rios, P.; Cecconi, F.; Pretre, A.; Dietler, G.; Michielin, O.; Piazza, F.; Juanico, B. Functional Dynamics of PDZ Binding Domains: a Normal-Mode Analysis., *Biophys. J.* **2005**, *89*, 14–21.

[41] Sharp, K.; Skinner, J. J. Pump-Probe Molecular Dynamics as a Tool for Studying Protein Motion and Long Range Coupling, *Proteins* **2006**, *65*, 347–361.

[42] Dhulesia, A.; Gsponer, J.; Vendruscolo, M. Mapping of Two Networks of Residues that Exhibit Structural and Dynamical Changes upon Binding in a PDZ Domain Protein., *J. Am. Chem. Soc.* **2008**, *130*, 8931–8939.

[43] Kong, Y.; Karplus, M. Signaling Pathways of PDZ2 Domain: a Molecular Dynamics Interaction Correlation Analysis., *Proteins* **2009**, *74*, 145–154.

[44] Gerek, Z. N.; Ozkan, S. B. Change in Allosteric Network Affects Binding Affinities of PDZ Domains: Analysis Through Perturbation Response Scanning., *PLoS Comput. Biol.* **2011**, *7*, e1002154.

[45] Cilia, E.; Vuister, G. W.; Lenaerts, T. Accurate Prediction of the Dynamical Changes within the Second PDZ Domain of PTP1e., *PLoS Comput. Biol.* **2012**, *8*, e1002794.

[46] Lockless, S. W.; Ranganathan, R. Evolutionarily Conserved Pathways of Energetic Connectivity in Protein Families, *Science* **1999**, *286*, 295–299.

[47] Suel, G. M.; Lockless, S. W.; Wall, M. A.; Ranganathan, R. Evolutionarily Conserved Networks of Residues Mediate Allosteric Communication in Proteins, *Nat. Struct. Biol.* **2003**, *10*, 59–69.

[48] Chi, C. N.; Elfström, L.; Shi, Y.; Snäll, T.; Engström, A.; Jemth, P. Reassessing a Sparse Energetic Network Within a Single Protein Domain, *Proc. Natl. Acad. Sci. USA* **2008**, *105*, 4679–4684.

[49] Burns, D. C.; Zhang, F.; Woolley, G. A. Synthesis of 3,3'-bis(Sulfonato)-4,4'-bis(Chloroacetamido)azobenzene and Cysteine Cross-Linking for Photo-Control of Protein Conformation and Activity., *Nat. Protoc.* **2007**, *2*, 251–258.

[50] Hamm, P.; Kaindl, R. A.; Stenger, J. Noise Suppression in Femtosecond Mid-Infrared Light Sources, *Opt. Lett.* **2000**, *25*, 1798–1800.

[51] Volkov, V.; Schanz, R.; Hamm, P. Active Phase Stabilization in Fourier-Transform Two-Dimensional Infrared Spectroscopy, *Opt. Lett.* **2005**, *30*, 2010–2012.

[52] Middleton, C. T.; Strasfeld, D. B.; Zanni, M. T. Polarization Shaping in the Mid-IR and Polarization-Based Balanced Heterodyne Detection with Application to 2D IR Spectroscopy,

Opt. Express **2009**, *17*, 14526–14533.

[53] Bloem, R.; Garrett-Roe, S.; Strzalka, H.; Hamm, P.; Donaldson, P. Enhancing Signal Detection and Completely Eliminating Scattering Using Quasi-Phase-Cycling in 2D IR Experiments, *Opt. Express* **2010**, *18*, 27067–27078.

[54] Johnson, P. J. M.; Koziol, K. L.; Hamm, P. Intrinsic Phasing of Heterodyne-Detected Multidimensional Infrared Spectra, *Opt. Express* **2017**, *25*, 2928–2938.

[55] Pronk, S.; Páll, S.; Schulz, R.; Larsson, P.; Bjelkmar, P.; Apostolov, R.; Shirts, M. R.; Smith, J. C.; Kasson, P. M.; Van Der Spoel, D.; et al. GROMACS 4.5: A High-Throughput and Highly Parallel Open Source Molecular Simulation Toolkit, *Bioinformatics* **2013**, *29*, 845–854.

[56] Hornak, V.; Abel, R.; Okur, A.; Strockbine, B.; Roitberg, A.; Simmerling, C. Comparison of Multiple Amber Force Fields and Development of Improved Protein Backbone Parameters, *Proteins* **2006**, *65*, 712–725.

[57] Best, R. B.; Hummer, G. Optimized Molecular Dynamics Force Fields Applied to the Helix-Coil Transition of Polypeptides, *J. Phys. Chem. B* **2009**, *113*, 9004–9015.

[58] Larsen, K. L.; Piana, S.; Palmo, K. Improved Side-Chain Torsion Potentials for the Amber ff99SB Protein Force Field, *Proteins* **2010**, *78*, 1950–1958.

[59] Jorgensen, W. L.; Chandrasekhar, J.; Madura, J. D.; Impey, R. W.; Klein, M. L. Comparison of Simple Potential Functions for Simulating Liquid Water, *J. Chem. Phys.* **1983**, *79*, 926–935.

[60] Joung, I. S.; Cheatham, T. E. Determination of Alkali and Halide Monovalent Ion Parameters for Use in Explicitly Solvated Biomolecular Simulations, *J. Phys. Chem. B* **2008**, *112*, 9020–9041.

[61] Wang, J.; Wang, W.; Kollman, P. A.; Case, D. A. Automatic Atom Type and Bond Type Perception in Molecular Mechanical Calculations, *J. Mol. Graph. Model.* **2006**, *25*, 247–260.

[62] Frisch, M. J.; Trucks, G. W.; Schlegel, H. B.; Scuseria, G. E.; Robb, M. A.; Cheeseman, J. R.; Scalmani, G.; Barone, V.; Mennucci, B.; Petersson, G. A.; et al., *Gaussian 09;* Gaussian Inc. Wallingford CT, 2009.

[63] Hess, B.; Kutzner, C.; Van Der Spoel, D.; Lindahl, E. GROMACS 4: Algorithms for Highly Efficient, Load-Balanced, and Scalable Molecular Simulation, *J. Chem. Theory Comput.* **2008**, *4*, 435–447.

[64] Darden, T.; York, D.; Pedersen, L. Particle Mesh Ewald: An Nlog(N) Method for Ewald Sums in Large Systems, *J. Chem. Phys.* **1993**, *98*, 10089–10092.

[65] Bussi, G.; Donadio, D.; Parrinello, M. Canonical Sampling Through Velocity Rescaling, *J. Chem. Phys.* **2007**, *126*, 014101.

[66] Berendsen, H. J. C.; Postma, J. P. M.; van Gunsteren, W. F.; DiNola, A.; Haak, J. R. Molecular Dynamics with Coupling to an External Bath, *J Chem Phys* **1984**, *81*, 3684–3690.

[67] Ernst, M.; Sittel, F.; Stock, G. Contact- and Distance-Based Principal Component Analysis of Protein Dynamics, *J. Chem. Phys.* **2015**, *143*, 244114.

[68] Steinhauser, O. Reaction Field Simulation of Water, *Mol. Phys.* **1982**, *45*, 335–348.

[69] Wolf, S.; Freier, E.; Cui, Q.; Gerwert, K. Infrared Spectral Marker Bands Characterizing a Transient Water Wire Inside a Hydrophobic Membrane Protein, *J. Chem. Phys.* **2014**, *141*, 22D524.

[70] Lee, C.; Yang, W.; Parr, R. G. Development of the Colle-Salvetti Correlation-Energy Formula into a Functional of the Electron Density, *Phys. Rev. B* **1988**, *37*, 785–789.

[71] Becke, A. D. Density-Functional Thermochemistry III: the Role of Exact Exchange, *J. Chem. Phys.* **1993**, *98*, 5648–5652.

[72] Johnson, III, R. D. NIST 101. Computational Chemistry Comparison and Benchmark Database, *CCCBDBD Computational Chemistry Comparison and Benchmark Database* **1999**.

[73] Mulliken, R. S. Electronic Population Analysis on LCAO–MO Molecular Wave Functions. I, *J. Chem. Phys.* **1955**, *23*, 1833–1840.

[74] Moses, J. E.; Moorhouse, A. D. The Growing Applications of Click Chemistry, *Chem. Soc. Rev.* **2007**, *36*, 1249–1262.

TOC Graphic

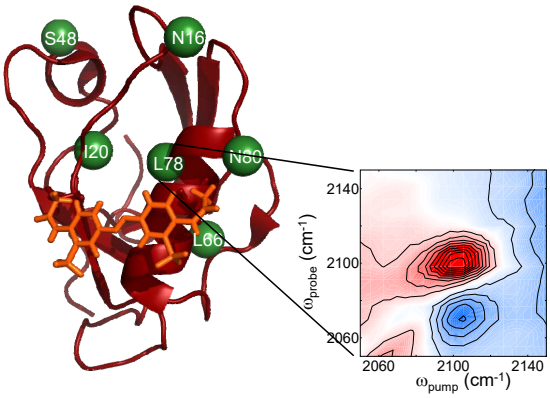
S48
N16
I20
L78
N68
L66
2140
2100
2060
ω_{probe} (cm^{-1})
2060
2100
2140
ω_{pump} (cm^{-1})